

A comparative performance ranking of some phosphonates and environmentally friendly polymers on CaCO₃ scaling inhibition by NACE protocol

Konstantin Popov*, Galina Rudakova, Vladimir Larchenko, Mariya Tusheva, Elena Afanas'eva, Svetlana Kombarova, Semen Kamagurov, Natalya Kovaleva

PJSC "Fine Chemicals R&D Centre", Moscow, 107258, Russia, Tel. +7 916 29174 81; emails: ki-popov@mtu-net.ru (K. Popov), rudakova@travers.su (G. Rudakova), larchenkove@mail.ru (V. Larchenko), tusheva@travers.su (M. Tusheva), lenaafanasyeva@mail.ru (E. Afanas'eva), kombarsv@yandex.ru (S. Kombarova), kamagurov@mail.ru (S. Kamagurov), n.e.kovaleva@gmail.com (N. Kovaleva)

Received 24 March 2016; Accepted 16 June 2016

ABSTRACT

A comparative ability of industrial samples of four phosphorus-free polymers (polyaspartate [PASP]; polyepoxysuccinate [PESA]; polyacrylic acid sodium salt [PAAS]; and copolymer of maleic and acrylic acid [MA-AA]) and of two phosphonates (aminotris(methylenephosphonic acid), ATMP; 1-hydroxyethane-1,1-bis(phosphonic acid), HEDP) to inhibit calcium carbonate precipitation is tested following the National Association of Corrosion Engineers (NACE) Standard TM0374-2007 for the dosages ranging from 1 to 25 mg·dm⁻³. In a parallel way, an aqueous phase is studied by dynamic light scattering (DLS), while the solid calcium carbonate is characterized by scanning electron microscopy and powder X-ray diffraction (XRD). The following ranking ATMP > HEDP > PESA (400–1,500 Da) ~ PASP (1,000–5,000 Da) > PAAS (3,000–5,000 Da) ~ MA-AA is found. DLS exhibits the formation of CaCO₃ particles with a particle size around 300–400 nm in the blank solution as well as in presence of all antiscalants immediately after a supersaturated solution preparation with negative ζ-potential around –5 mV for all reagents. Only for MA-AA the bigger aggregates are formed. XRD analysis revealed calcite formation at low dosages of all antiscalants, although the crystal shapes are distorted. At a higher concentration of some antiscalants, aragonite (PAAS, ATMP) and vaterite (PASP) are found to be the dominating crystal modifications. The differences between the blank experiments and scaling in the presence of inhibitor are attributed neither to CaCO₃ particle size nor to electrostatic charge, but to the number of particles formed. In presence of an antiscalant, the number of solid phase particles is sufficiently less, than in a blank solution. Thus, both the polymers and phosphonates prevent mostly the formation of initial crystallization centers under NACE protocol conditions.

Keywords: Scale inhibition; Calcium carbonate; Biodegradable polymers; Phosphonates; NACE; DLS; SEM; XRD

1. Introduction

Scale formation in upstream oil and gas industry, reverse osmosis desalination processes, steam generators, boilers,

cooling water towers and pipes is a serious problem, causing significant plugging of wells, pipelines, membranes, and increasing the production cost [1–4]. A widely used technique for controlling scale deposition is an application of chemical inhibitors [1,2]. Commonly used commercial antiscalants are represented by three chemical families: polyphosphates

*Corresponding author.

Presented at the EDS conference on Desalination for the Environment: Clean Water and Energy, Rome, Italy, 22–26 May 2016.

(hexametaphosphate [HMP], tripolyphosphate [TPP], etc.), organophosphonates (aminotris(methylenephosphonic acid) [ATMP]; 1-hydroxyethane-1,1-bis(phosphonic acid) [HEDP]; 2-phosphonobutane 1,2,4-tricarboxylic acid [PBTC]; ethylenediaminetetra(methylenephosphonic acid) [EDTPH], etc.) and organic polyelectrolytes (polyacrylates [PA], polycarboxysulfonates [PCS]). Among these, the organophosphonates are dominating recently at the world market [5]. At the same time, phosphorus-based inhibitors are hardly biodegradable. These reagents persist for many years after their disposal, which leads to eutrophication problems. Phosphorus discharges are, therefore, regulated in many countries worldwide, and permissible limits are constantly decreasing [6].

The environmental concerns and discharge limitations have forced the scale-inhibitor chemistry to move toward “green antiscalants” that are readily biodegradable and have minimal environmental impact [3,6,7]. Intensive efforts are applied recently to develop the “green” alternatives to organophosphonates and nonbiodegradable PA [7–9]. Among these novel inhibitors, chemicals such as polymaleates (PMA), polyaspartates (PASP), polyepoxysuccinates (PESA), carboxymethylinulin biopolymer (CMI) and other polysaccharides, as well as their various derivatives, including copolymers with PA, are worthwhile to mention [3,4,6,7,10–16].

It is important to note that the new antiscalants should have acceptable levels of performance at cost-effective dose rates. This requirement raises a problem of reliable tests, which permit a correct “old red” and “novel green” inhibitors efficiency comparison. Unfortunately, most of the data published on CaCO₃ deposition are considering a single antiscalant studied under hardly comparable conditions, e.g., different CaCO₃ supersaturation index, brine composition, temperature, pH, measurement technique, etc. The known comparative performance ranking reports done by one and the same group are rare. At the same time, such rankings give frequently rather conflicting results. For example, different research groups report for CaCO₃ deposits the reversed antiscalant efficacy sequences. Particularly for the traditional reagents HEDP and PA, and for the novel PESA and PMA, one group presents a ranking: HEDP > PESA (1,500 Da) > PMA (600 Da) > PA (1,800 Da) [15], while another one reports: PA (1,800 Da) > PMA (600 Da) > PESA (1,500 Da) [17,18]. Meanwhile for the pair HEDP/PA, the diversity of CaCO₃ antiscalant efficiency estimations is ranging from HEDP >> PA (1,800 Da) [15] to PA (2,000 Da) ~ HEDP [19], and even to HEDP < PA (2,000 Da) [20]. A similar inconsistency is observed for HEDP and ATMP: ATMP >> HEDP [21], ATMP ~ HEDP [22] and ATMP << HEDP [23].

In this respect, a comparative performance of some traditional antiscalants (phosphonates, PA) and the novel environmentally friendly polymers studied by a reliable method under comparable conditions becomes actual. In the present work, the effects of four industrial samples of phosphorus-free polymers and of two phosphonates were tested with respect to their ability to inhibit calcium carbonate precipitation following NACE Standard [24]. Since it is anticipated that the inhibitors would cause changes of the CaCO₃ particles surface charge, thus affecting their aggregation [3], then the zeta-potential measurements by dynamic light scattering technique were conducted.

2. Materials and methods

2.1. Materials

Polymer-based industrial antiscalants polyaspartic acid sodium salt (PASP), copolymer of maleic and acrylic acid (MA-AA), polyepoxysuccinic acid (PESA) and sodium salt of polyacrylic acid (PAAS) have been kindly supplied by Shandong Taihe Water Treatment Co., Ltd., Shandong, China, and analyzed by Nuclear Magnetic Resonance (NMR) and dynamic light scattering (DLS) technique. Polymer stock solutions were prepared on a dry weight basis. The desired concentrations of the polymers were obtained by dilution. Table 1 lists the properties of polymers tested.

Industrial solid phosphonates, ATMP and HEDP, have been supplied by a manufacturer OAO “Khimprom”, Novocheboksarsk, Russia. Both have been analyzed by NMR, found to have nearly reagent grade purity and used without further purification. Phosphonate stock solutions were prepared on a dry weight basis. The desired concentrations of polymers were obtained by dilution.

¹H, ³¹P and ¹³C NMR measurements of polymer aqueous solutions were recorded with Bruker AVANCE II 300 spectrometer at ambient temperature in the 5-mm-diameter sample tubes. The external standard solutions of TMS (¹H, ¹³C) or phosphoric acid (³¹P) were placed in a 1-mm inner coaxial tube.

For brine preparations, the analytical grade chemicals were used. Stock solutions of calcium chloride, sodium carbonate, sodium chloride and magnesium chloride were prepared from the respective crystalline solids (Sigma-Aldrich Corp., St. Louis, Missouri, US; EKOS-1) using distilled water, filtered through a 0.22-μm filter paper and standardized as described in [24].

2.2. Inhibition evaluation protocol

Inhibition tests were run following the NACE Standard TM0374-2007 protocol [24]. Two synthetic brines were prepared with distilled water: calcium-containing brine (12.15 g·dm⁻³ CaCl₂·2H₂O; 3.68 g·dm⁻³ MgCl₂·6H₂O; 33.0 g·dm⁻³ NaCl) and bicarbonate-containing brine (7.36 g·dm⁻³ NaHCO₃; 33.0 g·dm⁻³ NaCl) saturated by CO₂. Being mixed at 1:1 volume ratio, these brines give a supersaturated calcium carbonate solution: 6.07 g·dm⁻³ (6,070 ppm) CaCl₂·2H₂O, 1.84 g·dm⁻³ (1,840 ppm) MgCl₂·6H₂O, 3.68 g·dm⁻³ (3,680 ppm) NaHCO₃ and 33.0 g·dm⁻³ (33,000 ppm) NaCl. The ionic strength of this solution provided mostly by NaCl by the end of the precipitation process was around 0.71 mol·dm⁻³, with activity coefficients γ_± = 0.68 [25]. The precipitation of salts from supersaturated solution depends on the saturation index *SI*, defined as Eq. (1):

$$SI = IAP / K^{\circ}_s \quad (1)$$

where *IAP* denotes the ion activity product, and *K*[°]_{*s*} is the thermodynamic solubility product of the salt considered.

Supersaturated solution of calcium carbonate with a calculated amount of inhibitor (from 2 to 25 mg·dm⁻³ for polymers, and from 1 to 10 mg·dm⁻³ for phosphonates) was

Table 1
Polymers studied as scale inhibitors in calcium carbonate supersaturated solutions

Reagent	Reagent formula	Appearance	Solid content, %	Molecular Mass, Da	pH, 1% water solution
PESA	<p>M=Na, R=H</p>	Amble transparent liquid	40.27	400–1,500	11.56
PASP	<p>m > n</p>	Umber liquid	40.94	1,000–5,000	9.81
MA-AA	<p>Free monomer as MA ≤ 9%</p>	Brown transparent liquid	48.80	Not specified	2.17
PAAS	<p>Free monomer as CH₂=CHCOOH ≤ 1%</p>	White powder	92.49	3,000–5,000	6.92

then kept for 24 h at 71°C, cooled and analyzed for residual calcium content by Ethylenediaminetetraacetic acid (EDTA) titration. The pH of the solutions at 25°C was about 7. All experiments were run in duplicates. The high *SI* values provided better accuracy of calcium content measurements and a good agreement between duplicate run results.

The performance of the tested compounds as calcium carbonate antiscalants was calculated (Eq. (2)) as inhibition percentage (*I*, %):

$$\text{Percent inhibition } (I, \%) = 100 \times \frac{[\text{Ca}]_{\text{exp}} - [\text{Ca}]_{\text{final}}}{[\text{Ca}]_{\text{init}} - [\text{Ca}]_{\text{final}}} \quad (2)$$

where $[\text{Ca}]_{\text{exp}}$ is the concentration of calcium in the filtrate in the presence of an inhibitor at 24 h; $[\text{Ca}]_{\text{final}}$ is the concentration of calcium in the filtrate in the absence of an inhibitor at 24 h; and $[\text{Ca}]_{\text{init}}$ is the concentration of calcium at the beginning of the experiment.

At the end of experiments, solid samples of precipitates were collected for characterization by powder X-ray diffraction (XRD) and by scanning electron microscopy (SEM). Besides, the liquid phase was monitored by DLS technique before and after heating. The corresponding data are presented in Tables 2–6 and Figs. 1–4.

2.3. Crystal characterization

After being triply rinsed with deionised water and air drying at 50°C, the precipitated solids were characterized by SEM (Hitachi TM-3030) and powder XRD (Bruker D8 Advance diffractometer; Cu K α ; Ni-filter; LYNXEYE detector). The XRD phase identification was done with Joint Committee on Powder Diffraction Standards (JCPDS) database, and relative phase content was estimated with Topaz R software (Bruker AXS). The sample examinations by SEM were done at 15 kV accelerating voltage in a charge-up reduction mode with crystal phase located on a conducting double-sided tape.

2.4. Liquid phase characterization

Liquid phase was monitored by the DLS technique. DLS experiments were performed at 25°C with a commercial Malvern Nano ZS ($\lambda = 633$ nm, operating power 4 mVt) at $\Theta = 173^\circ$. The refractive index *n* (1.3375), the viscosity η (974, 2 μPa) and the density *d* (1,022 $\text{g}\cdot\text{dm}^{-3}$) of 0.6 $\text{mol}\cdot\text{dm}^{-3}$ NaCl aqueous solution were measured and used to characterize the solvent. All polymer solutions were clarified by 0.45 μm Millipore Nylon filters to remove dust. The same operation was done with calcium and carbonate solutions

Table 2
Polymer performance as a scale inhibitor in calcium carbonate supersaturated solution

Polymer	Initial polymer particles characteristics ^a		Polymer dosage, mg·dm ⁻³					
			10.0			25.0		
	Mean diameter, nm	ζ, mV	pH		I, % ^b	pH		I, % ^b
			Initial	Final		Initial	Final	
PASP	11 (3)	-12 (1)	7.2	6.9	89 ± 2	7.2	7.1	89 ± 2
PESA	108 (5)	-17 (1)	7.1	7.0	93 ± 1	7.1	7.2	100 ± 1
MA-AA	209 (50)	-20 (1)	7.2	6.9	84 ± 2	7.2	7.0	88 ± 2
PAAS	9 (2)	-14 (1)	7.4	6.9	83 ± 2	7.4	6.9	90 ± 2

^aHydrodynamic diameter values (by number) for 20 mg·dm⁻³ in 0.1 M NaNO₃ polymer aqueous solution; pH 8; data in parentheses represent standard deviation for three replicate measurements.

^bMean arithmetic values from two replicate runs.

Table 3
Phosphonate performance as a scale inhibitor in calcium carbonate supersaturated solution

Phosphonate	Phosphonate dosage, mg·dm ⁻³					
	1.0			3.0		
	pH		I, % ^a	pH		I, % ^a
Initial	Final	Initial		Final		
ATMP	7.10	6.70	82 ± 2	7.10	6.91	100 ± 1
HEDP	7.48	6.63	44 ± 1	7.42	6.93	100 ± 1

^aMean arithmetic values from two replicate runs.

before they have been mixed. The initial and final samples of calcium carbonate saturated solutions were analyzed for solid phase particle size and ζ-potential. The same was done for calcium-free samples of all polymers used.

3. Results and discussion

Fig. 1 demonstrates that all four polymers reveal an increasing inhibition performance as the dosage is changed from 2 to 15 mg·dm⁻³. At the same time when polymer concentration exceeds 15 mg·dm⁻³, then the efficacy becomes dosage-independent. For PESA, the constancy indicates that 100% efficiency is achieved. Meanwhile for MA-AA, PASP and PAAS, the maximal efficacy does not exceed 90%. A similar observation was also reported for PA [17,20,22,26] and PASP [27]. Polyacrylate-based inhibitors (MA-AA, PAAS) indicate the similar efficacy within the experimental error, Table 2. Therefore, in Fig. 1, the corresponding data are presented by a single curve (solid line). PASP indicates a slightly better performance at low dosage (<5 mg·dm⁻³), while PESA has evidently higher efficiency at a polymer content >15 mg·dm⁻³.

Phosphonates, HEDP and ATMP, demonstrate the same dosage dependence as PESA, Fig. 2. However, both provide 100% inhibition at the dosages already below 5 mg·dm⁻³. ATMP reveals generally better performance than HEDP, Table 3. On the other hand, both phosphonates look more efficient than MA-AA and PAAS and a bit better than PESA. In this respect, the following ranking becomes possible (Eq. (3)):

$$\begin{aligned} & \text{ATMP} > \text{HEDP} > \text{PESA}(400 - 1500 \text{ Da}) \\ & \sim \text{PASP}(1000 - 5000 \text{ Da}) > \text{PAAS}(3000 - 5000 \text{ Da}) \\ & \sim \text{MA-AA} \end{aligned} \quad (3)$$

Such a ranking is in a general agreement with those reported in [15,22,26,28], Table 4, and conflicts the results presented in [20,23]. It should also be noted that the purity of commercial reagents studied is different. The active substances content in solid phosphonates, ATMP and HEDP, is close to 95% ÷ 100%, while a significant part of polymer mass indicated by a manufacturer is constituted by the impurities of monomers and oligomers. These are likely to be a ballast, which diminishes the “true” efficiency of polymer itself. In this respect, PESA may be treated as a reagent quite comparable with ATMP and HEDP.

The observed shape of the curves at Figs.1 and 2 is typical for antiscalants: an efficiency is rapidly increasing with a corresponding increase of a reagent concentration, and then becomes dosage independent when 100% inhibition is achieved [3,15,16,17,26–30]. Our data for ATMP, HEDP and PESA fit well this scheme. However, along with such an obvious “regular” trend some cases are registered, when the dosage independence is reached far below the 100% inhibition level [15,17,26,30].

In the present work, such “irregular” behavior is found for PAAS, MA-AA and PASP. A possible explanation to an anomalously low efficiency limit might be a self-association of some polymer molecules at higher dosages relative to the diluted solutions. Indeed for PAAS, we have found in a

Table 4
Scale inhibitors ranking reports for calcium carbonate

Experiment details ^a	Dosage, mg·dm ⁻³ (ppm)	Ranking	Ref.
Static method. Brine composition: CaCl ₂ •2H ₂ O (0.006 mol·dm ⁻³); NaHCO ₃ (0.012 mol·dm ⁻³); pH = 9; 10 h at 80°C	10	PBTC > HEDP > PESA (1,500 Da) > PMA (600 Da) > PA (1,800 Da)	[15]
Static method. Brine composition: CaCl ₂ •2H ₂ O (0.006 mol·dm ⁻³); NaHCO ₃ (0.004 mol·dm ⁻³); pH is not specified; 10 h at 60°C	10	PA (1,800 Da) > PMA (600 Da) > PESA (1,500 Da)	[17]
	16	PESA (1,500 Da) > PMA (600 Da) ~ PA (1,800 Da)	
Static method. Brine composition, PMA molecular mass and pH are not specified; 18 h at 70°C	0.5	PA (2,000 Da) > HEDP > PA (5,000 Da) > PMA > HEDP > PA	[20]
Static method. Brine composition: [Ca ²⁺] (0.015 mol·dm ⁻³); [Mg ²⁺] (0.008 mol·dm ⁻³); [HCO ₃ ⁻] (0.010 mol·dm ⁻³); pH = 9; 3 h at 44°C	5	ATMP ~ HEDP > PBTC > PA (5,000 Da)	[22]
	10	PBTC > ATMP ~ HEDP > PA (5,000 Da)	
	20	HEDP ~ PBTC > ATMP ~ PA (5,000 Da)	
Static method. Brine composition: CaCl ₂ •2H ₂ O (0.006 mol·dm ⁻³); NaHCO ₃ (0.012 mol·dm ⁻³); pH = 7; 10 h at 60°C	10	PBTC > HEDP > PESA (1,500 Da) > PA (1,800 Da)	[26]
Dynamic method. Calcite seed crystal growth rate measurement in a solution [Ca ²⁺] = [HCO ₃ ⁻] = 0.01 mol·dm ⁻³ at 25°C; pH 9.2	2.5	HEDP > EDTPH > ATMP	[23]
Static method. Brine composition: CaCl ₂ •2H ₂ O; NaHCO ₃ ; pH 8.2; 20 h at 66°C	3	PMA (<1,000 Da) > PA (6,000 Da)	[3]
Static method. Brine composition: CaCl ₂ •2H ₂ O (0.0125 mol·dm ⁻³); NaHCO ₃ (0.0125 mol·dm ⁻³); pH = 9; 8 h at 80°C	10	PESA (400–1,500 Da) > PASP (1,000–5,000 Da)	[27]
Static method. Bubbling of air through a brine with [Ca ²⁺] = 0.0064 mol·dm ⁻³ and [HCO ₃ ⁻] = 0.012 mol·dm ⁻³ ; 5 h at 60°C; pH is not specified	10	ATMP > PA (2,000 Da)	[28]
	20	PA (2,000 Da) > ATMP	
Static method. Brine composition: CaCl ₂ •2H ₂ O (0.041 mol·dm ⁻³); MgCl ₂ •6H ₂ O (0.009 mol·dm ⁻³); NaHCO ₃ (0.044 mol·dm ⁻³); NaCl (0.57 mol·dm ⁻³); pH 6 ÷ 7; 24 h at 71°C	10	ATMP > HEDP > PESA (400–1,500 Da) ~ PASP (1,000–5,000 Da) > PAAS (3,000–5,000 Da) ~ MA-AA	Present study

^aIf not specially specified, the inhibition degree estimation is based on the initial and residual calcium content measurement by EDTA titration.

20 mg·dm⁻³ solution a fraction with a size ~4,000 nm. But for MA-AA and PASP, a bigger aggregates were not registered.

A set of experiments with an antiscalant dosage of 1–10 mg·dm⁻³ was chosen for an equilibrium between liquid and solid phases characterization. The precipitated phases are identified by XRD, Table 5. In the absence of inhibitors, calcite is the main crystal form of calcium carbonate found for the brine used in this study. The second form identified in the scale was aragonite. This result is consistent with those found earlier for calcium carbonate supersaturated solution [31–34] and with the higher thermodynamic stability of calcite relative to the other polymorphic forms of calcium carbonate at ambient temperature [17,33]. Besides, some impurities of NaCl crystals arising from the supporting electrolyte of the brine are also found in our case. These are not demonstrated in Table 5. The corresponding SEM images of calcium carbonate crystals exhibit regular rhombohedron or cubic shape, typical for aragonite, with an average particle size of about 20–40 μm, Fig. 3(a).

Small dosages of antiscalants ranging from 1 to 5 mg·dm⁻³ do not affect the solid phase composition, Table 5. In the presence of polymers and phosphonates, the

Table 5
XRD calcium carbonate scale characterization results

Sample	Inhibitor concentration, mg·dm ⁻³	Solid phase composition ^a , %		
		Calcite	Aragonite	Vaterite
Blank	0	82	18	0
PESA	1	100	0	0
	5	100	0	0
PAAS	5	13	77	10
	10	40	60	0
MA-AA	1	100	0	0
	5	100	0	0
PASP	5	100	0	0
	10	6	41	53
ATMP	1	100	0	0
	5	18	82	0
HEDP	5	82	18	0

^aThe accuracy of a relative particular phase content is within 10%–15%.

Table 6

Calcium carbonate particles characterization in an aqueous phase at 25°C after 24 h at 70°C of a supersaturated solution treatment^a

Scale inhibitor	Blank	PESA	PAAS	MA-AA	PASP	ATMP	HEDP
Inhibitor dosage, mg·dm ⁻³	0	10	10	10	10	10	10
Scale inhibition, %	0	93	83	84	89	100	100
pH	6.4	7.1	7.0	7.2	7.0	7.2	7.2
Mean hydrodynamic Diameter (by volume), nm:							
immediately after supersaturated solution preparation	320 (50)	270 (50)	270 (50)	580 (100)	240 (50)	340 (50)	670 (80)
after 24 h incubation	178 (40)	430 (60)	400 (50)	1,900 (100)	420 (50)	490 (50)	530 (80)
ζ-potential, mV: immediately after supersaturated solution preparation	-13 (2)	-10 (1)	-10 (1)	-10 (1)	-11(1)	-10 (1)	-6 (1)
after 24 h incubation	-7 (2)	-5 (1)	-10 (1)	-10 (1)	-10 (1)	-8 (1)	-3 (1)

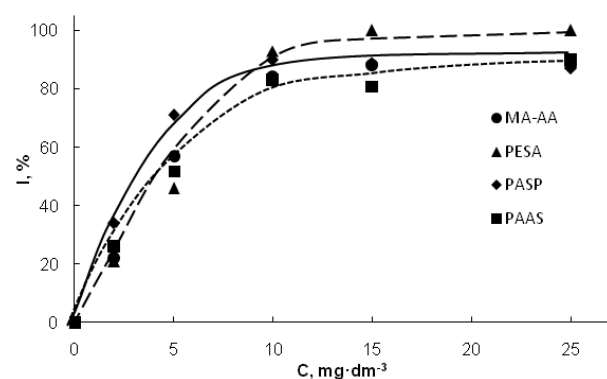
^aData in parentheses represent standard deviation for three replicate measurements.

Fig. 1. Inhibition of calcium carbonate precipitation in the presence of varying concentration (C) of polymers.

calcium carbonate solid phase represents either calcite or calcite and aragonite binary mixture. For the samples with 5 mg·dm⁻³ of PESA, MA-AA, PASP and HEDP, the calcite is dominating in a solid phase, while for PAAS and ATMP the formation of aragonite is more preferable.

At the same time, the SEM images indicate that all antiscalants change the morphology of calcite crystals to irregular shapes, Fig. 3. Both PESA and PASP at the dosages from 1 to 5 mg·dm⁻³ support the calcite formation, Table 5, but the calcite crystals in the presence of these antiscalants get distorted (Figs. 3(b) and (c)) relative to the calcite crystals formed in the blank solution (Fig. 3(a)). At a higher inhibitor concentration, the crystal distortion becomes even more pronounced, although the crystal form composition is also changed, Fig. 4. For example, both phosphonates provide a needle-like shape (Figs. 3(e) and (f)), while PESA application results in the spherical crystals (Fig. 3(b)). Evidently, such a crystal morphology change is caused by a nonuniform sorption of inhibitor molecules on the different crystal active sides. Such a poisoning of crystal surfaces by antiscalants leads to the inhibition of the further crystal growth and is recognized as a main ground for microcrystals deposition prevention [17,27,35].

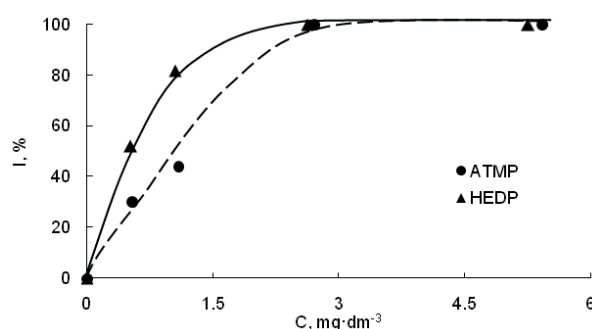


Fig. 2. Inhibition of calcium carbonate precipitation in the presence of varying concentration (C) of phosphonates.

An increase of the inhibitor dosage up to 10 mg·dm⁻³ diminishes the amount of scale. Therefore, for ATMP, HEDP, PESA and MA-AA, an isolation of solid phase quantities suitable for XRD analysis was hardly possible. However, for PAAS and PASP, such an analysis was performed, Table 5. The results indicate clearly that the presence of antiscalant impacts not only the morphology, but also the polymorph form of calcium carbonate crystals. Indeed, at higher concentration, PAAS provides preferably aragonite than calcite formation, Table 5.

Meanwhile, PASP application leads to the formation of calcite, aragonite and vaterite phases mixture. Among these, the vaterite becomes a dominating one. Vaterite is the initial phase known to be formed from CaCO₃ supersaturated solutions [33,34]. Then in the absence of inhibitors, vaterite is transformed into a more stable calcite [36]. Therefore, the thermodynamically unstable vaterite and aragonite could be stabilized kinetically in the presence of certain amount of PASP, Table 5. A similar result of the least stable calcium carbonate form stabilization was registered for PASP [27], PESA [27], some other polymers [17,26,37] and EDTA [31].

One research group has found a strong dependence of calcite/aragonite/vaterite ratio on the phosphonate dosage (HEDP, PBTC, ATMP) [38]. However, we can't confirm the same for HEDP and ATMP, although the experimental

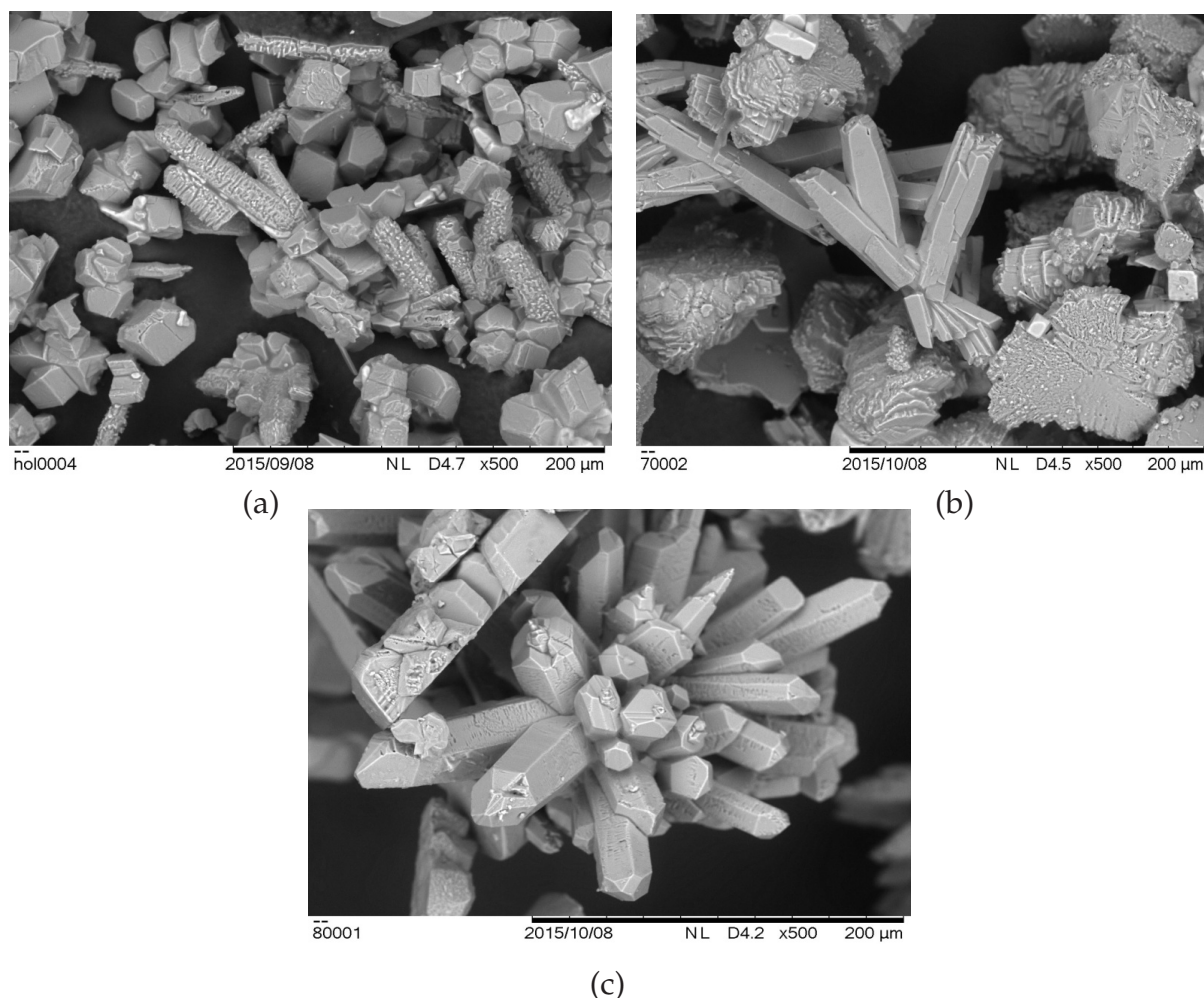


Fig. 3. SEM images (x500) of calcium carbonate crystals: in the absence of inhibitor (a) and in the presence of $1.0 \text{ mg}\cdot\text{dm}^{-3}$ PESA (b) and PASP (c).

conditions of the present work and of the experiments performed in [38] are very close to each other. In our case, both phosphonates revealed only calcite phase in equilibrium with brine until 100% inhibition is achieved.

Along with solids characterization, the DLS experiments for the liquid phase were performed, Table 6. These experiments were run for a $10 \text{ mg}\cdot\text{dm}^{-3}$ antiscalant dosage, which provides either 100% (ATMP, HEDP, PESA) or nearly 90% (PASP, PAAS, MA-AA) inhibition. Each supersaturated calcium carbonate solution was tested before and after 24 h incubation at 70°C , and a subsequent cooling the sample to 25°C .

Immediately after supersaturated solution preparation, a blank solution reveals the presence of rather large calcium carbonate particles, characterized by 300–400 nm mean diameter and ζ -potential of around -13 mV , Table 6. The latter is provided by an excess of carbonate ions relative to calcium cations in the system studied. This colloidal solution is very unstable and within the next 24 h at ambient temperature the corresponding increase in the scale mass is observed, while the particle dimensions are diminished to 180 nm due to the aggregation and scaling of the bigger size fractions. Meanwhile the ζ -potential changes to -8 mV . Probably a decrease of ζ -potential absolute value is associ-

ated with calcium and magnesium ions adsorption onto a negatively charged solid calcium carbonate surface.

The high temperature treatment of the blank solution leads to the particle aggregation and scaling. The mean particle size in a liquid phase is reduced to c.a. $150 \div 180 \text{ nm}$, e.g., the bigger particles are preferably deposited. ζ -potential is diminished from -13 to -7 mV .

For PESA, PAAS, PASP and ATMP, immediately after the supersaturated solution preparation, a formation of 200–300 nm diameter particles is registered. This is very similar to the blank solution. At the same time HEDP and MA-AA reveal much bigger aggregates: 670 and 580 nm correspondingly. An exceptionally high hydrodynamic diameter of solid particles in MA-AA solutions is likely to be explained by a specific “calcium carbonate–MA-AA” aggregate formation as far as MA-AA itself exhibits rather large globules, Table 2. All these particles reveal negative electrostatic charge with ζ -potential around -10 mV , provided either by carbonate anions, or/and by the free negatively charged groups of the antiscalant (carboxylate of phosphonate group).

After 24 h of treatment at 71°C with PESA, PASP, ATMP, MA-AA and PAAS, the supersaturated calcium carbonate

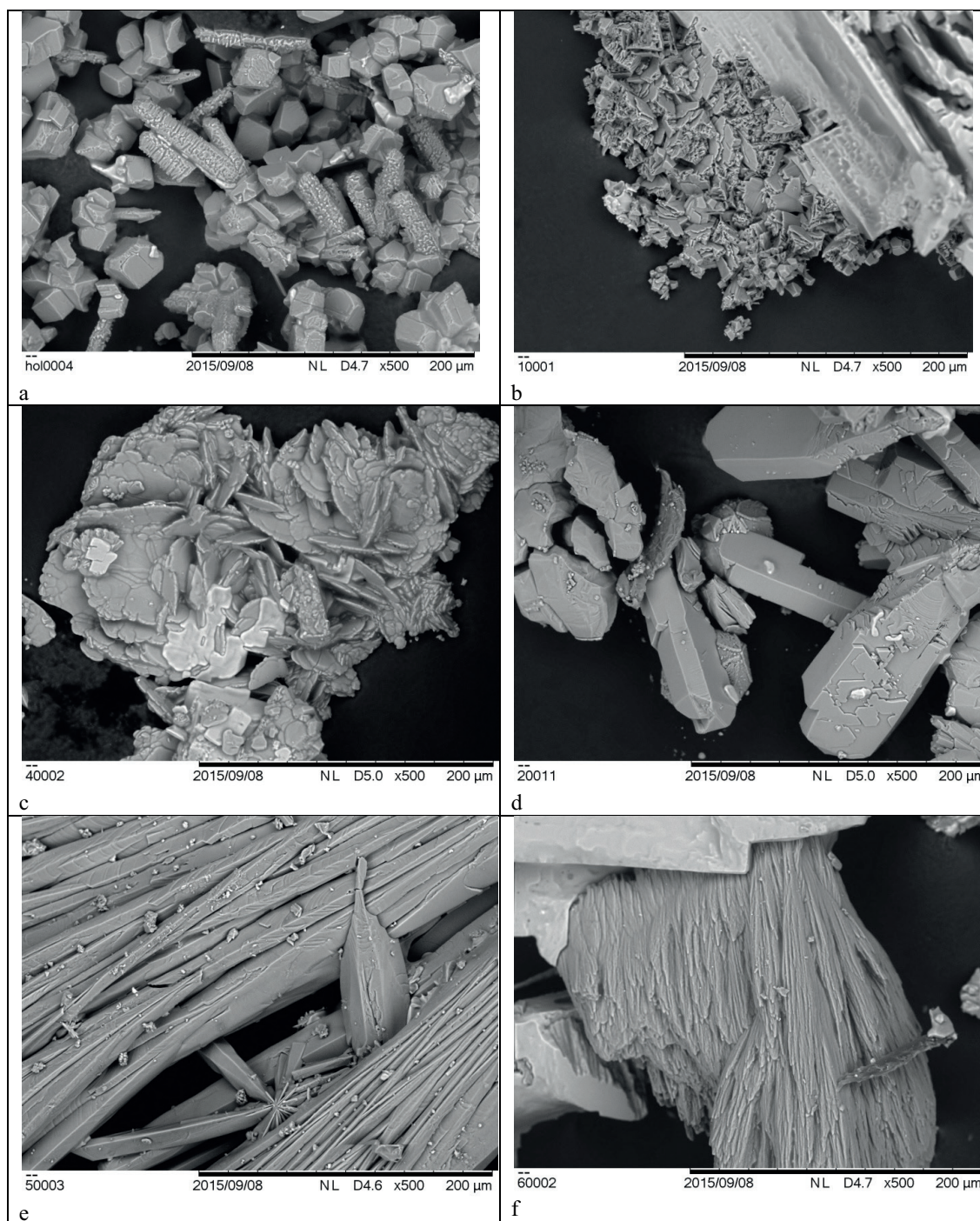


Fig. 4. SEM images (x500) of calcium carbonate crystals: in the absence of inhibitor (a) and in the presence of $10 \text{ mg} \cdot \text{dm}^{-3}$ PESA (b), PASP (c), PAAS (d), ATMP (e), and HEDP (f).

solutions exhibit a significant particles size growth and a small decrease, if any, in ζ -potential values. However, this growth is not followed by a corresponding bulk solid phase formation. For HEDP solutions, no size change is observed. The details of the calcium carbonate particles enlargement mechanism is a matter of further study. Evidently, a poisoning of crystal surfaces growth by the antiscalants is not the main ground of the bulk scale formation inhibition in this case.

The ζ -potential values are in a reasonable agreement with those found earlier for CaCO_3 stabilized by PA [39,40] and phosphonates [41]. However, the observed ζ -potentials are hardly capable to stabilize the colloidal solution, which requires normally $30 \text{ mV} \leq \zeta$ or $\zeta \leq -30 \text{ mV}$ [40]. Therefore, ζ is also unlikely to provide colloidal stability of calcium carbonate under the conditions of a NACE protocol.

Therefore, the differences between the blank experiments and scaling in the presence of inhibitor are not associated with either CaCO_3 particle size or electrostatic charge, but with the number of particles formed. Tentatively, in the latter case, the number of solid phase particles is sufficiently less, than in a blank solution. Thus, both the polymers and phosphonates studied prevent mostly the initial crystallization centers formation.

4. Conclusions

A relative ability of industrial samples of four phosphorus-free polymers (PASP, PESA, PAAS, MA-AA) and of two phosphonates (ATMP, HEDP) to inhibit calcium carbonate precipitation is tested following the NACE Standard TM0374-2007 for the dosages ranging from 1 to 25 $\text{mg}\cdot\text{dm}^{-3}$. The following ranking $\text{ATMP} > \text{HEDP} > \text{PESA}$ (400 ÷ 1,500 Da) ~ PASP (1,000 ÷ 5,000 Da) > PAAS (3,000–5,000 Da) ~ MA-AA is found.

DLS exhibits the formation of CaCO_3 particles with a particle size around 300–400 nm in the blank solution as well as in presence of all antiscalants immediately after a super-saturated solution preparation. XRD analysis revealed the calcite formation at low dosages of all antiscalants, although the crystal shapes are distorted. At a higher concentrations of some antiscalants, the aragonite (PAAS, PASP) and vaterite (PASP) are found to be the dominating crystal modifications.

The differences between the blank experiments and scaling in the presence of inhibitor are likely to be associated with neither CaCO_3 particle size nor electrostatic charge, but with the number of initial particles formed. In presence of antiscalant, the number of solid carbonate phase particles is sufficiently less, than in a blank solution. Thus, both the polymers and phosphonates studied prevent mostly the initial crystallization centers formation.

Acknowledgments

This work was supported by the Ministry of Education and Science of the Russian Federation, Project ID RFME-F158214X0007, Project No. 14.582.21.0007.

References

- [1] K.I. Popov, N.E. Kovaleva, G. Ya. Rudakova, S.P. Kombarova, V.E. Larchenko, Recent state-of-the-art of biodegradable scale inhibitors for cooling-water treatment applications (review), *Therm. Eng.*, 63 (2016) 122–129.
- [2] J. MacAdam, S.A. Parsons, Calcium carbonate scale formation and control, *Rev. Environ. Sci. Biotechnol.*, 3 (2004) 159–169.
- [3] Z. Amjad, P.G. Koutsoukos, Evaluation of maleic acid based polymers as scale inhibitors and dispersants for industrial water applications, *Desalination*, 335 (2014) 55–63.
- [4] M.K. Jensen, M.A. Kelland, A new class of hyperbranched polymeric scale inhibitors, *J. Pet. Sci. Eng.*, 94–95 (2012) 66–72.
- [5] Scale Inhibitor Market by Type and by Application - Global Trends & Forecast to 2019. Available from: <http://www.researchandmarkets.com/reports/2933881/scale-inhibitor-market-by-type-and-by-application#pos-0>
- [6] D. Hasson, H. Shemer, A. Sher, State of the art of friendly “green” scale inhibitors: a review article, *Ind. Eng. Chem. Res.*, 50 (2011) 7601–7607.
- [7] M. Chaussemier, E. Pourmohtasham, D. Gelus, N. Pécou, H. Perrot, J. Lédion, H. Cheap-Charpentier, O. Horner, State of art of natural inhibitors of calcium carbonate scaling, *Desalination*, 356 (2015) 47–55.
- [8] M.M. Jordan, E. Sorhaug, D. Marlow, Red vs. green scale inhibitors for extending squeeze life – a case study from the North sea, Norwegian sector – part II, *SPE Production & Operations*, 27 (2012) 404–413.
- [9] K.D. Demadis, E. Neofotistou, E. Mavredaki, M. Tsikakis, E.-M. Sarigiannidou, S.D. Katarachia, Inorganic foulants in membrane systems: chemical control strategies and the contribution of “green chemistry”, *Desalination*, 179 (2005) 281–295.
- [10] N.M. Kumar, K. Kanny, A novel biodegradable poly(hydroxybutanedioic acid-co-2-hydroxypropane-1,2,3-tricarboxylic acid) copolymer for water treatment applications, *Open J. Organic Polym. Mater.*, 2 (2013) 53–58.
- [11] Y. Gao, L. Fan, L. Ward, Z. Liu, Synthesis of polyaspartic acid derivative and evaluation of its corrosion and scale inhibition performance in seawater utilization, *Desalination*, 365 (2015) 220–226.
- [12] L. Xinhua, W. Wenjing, T. Xinjia, D. Yunfei, Z. Xinqiang, S. Hong, Study of corrosion and scale inhibition of polyoxosuccinic acid derivative, *Asian J. Chem.*, 26 (2014) 7716–7720.
- [13] H. Zhang, F. Wang, X. Jin, Y. Zhu, A botanical polysaccharide extracted from abandoned corn stalks: modification and evaluation of its scale inhibition and dispersion performance, *Desalination*, 326 (2013) 55–61.
- [14] A. Benbaki, T. Bachir-Bey, Synthesis and characterization of maleic acid polymer for use as scale deposits inhibitors, *J. Appl. Polym. Sci.*, 116 (2010) 3095–3102.
- [15] Y. Liu, Y. Zhou, Q. Yao, J. Huang, G. Liu, H. Wang, K. Cao, Y. Chen, Y. Bu, W. Wu, W. Sun, Double-hydrophilic polyether antiscalant used as a crystal growth modifier of calcium scales in cooling-water systems, *J. Appl. Polym. Sci.*, 131 (2014) 39792/1-39792/12.
- [16] B. Zhang, J. Li, X. Lv, Y. Cui, Y. Xu, Synthesis of polyaspartic acid/2-amino-2-methyl-1,3-propanediol graft copolymer and evaluation of its scale inhibition and corrosion inhibition performance, *Desal. Wat. Treat.*, 54 (2014) 1998–2004.
- [17] M. Xue, G. Liu, Y. Zhou, H. Wang, J. Huang, Q. Yao, L. Ling, K. Cao, Y. Liu, Y. Bu, Y. Chen, W. Wu, W. Sun, Acrylic acid-allylpolyethoxy carboxylate copolymer: an effective and environmentally friendly inhibitor for carbonate and sulphate scales in cooling water systems, *Int. J. Green Energy*, 12 (2015) 1151–1158.
- [18] J. Huang, G. Liu, Y. Zhou, Q. Yao, Y. Yang, L. Ling, H. Wang, K. Cao, Y. Liu, P. Zhang, W. Wu, W. Sun, Acrylic acid-allylpolyethoxy carboxylate copolymer as an environmentally friendly calcium carbonate and iron(III) scale inhibitor, *Clean Technol. Environ. Policy*, 15 (2013) 677–685.
- [19] P.G. Klepetsanis, P.G. Koutsoukos, Z. Amjad, Calcium Carbonate and Calcium Phosphate Scale Formation and Inhibition at Elevated Temperature, Z. Amjad, Ed., *Advances in Crystal Growth Inhibition Technologies*, Kluwer Academic Publishers, New York, Boston, Dordrecht, London, Moscow, 2002, pp.139–149.
- [20] L.A. Perez, D.F. Zidovec, Scale Control by Using a New Non-Phosphorus, Environmentally Friendly Scale Inhibitor, Z. Amjad, Ed., *Mineral Scale Formation and Inhibition*, Springer Science+Business Media, New York, 1998, pp. 47–61.
- [21] R.V. Davis, P.W. Carter, M.A. Kamrath, D.A. Jonson, P.E. Reed, The Use of Modern Methods in the Development of Calcium Carbonate Inhibitors for Cooling Water System, Z. Amjad, Ed., *Mineral Scale Formation and Inhibition*, Springer Science+Business Media, New York, 1998, pp. 33–46.
- [22] K.D. Demadis, B. Yang, P.R. Young, D.L. Kouznetsov, D.G. Kelley, Rational Development of New Cooling Water Chemical Treatment Programs for Scale and Microbial Control, Z. Amjad, Ed., *Advances in Crystal Growth Inhibition Technologies*, Kluwer Academic Publishers, New York, Boston, Dordrecht, London, Moscow, 2002, pp. 215–234.
- [23] M.M. Reddy, G.H. Nancollas, Calcite crystal growth inhibition by phosphonates, *Desalination*, 12 (1973) 61–73.

- [24] NACE Standard TM0374-2007 (formerly TM0374-2001), Item No. 21208, Laboratory Screening Tests to Determine the Ability of Scale Inhibitors to Prevent the Precipitation of Calcium Sulfate and Calcium Carbonate from Solution (for Oil and Gas Production Systems), 2007.
- [25] Ionic Strength Corrections for Stability Constants using Specific Interaction Theory (SIT) for Windows 9x, NT, 2000, and xp, L.D. Pettit, Academic Software, IUPAC, 2003. Available on the IUPAC site: www.iupac.org and www.acadsoft.co.uk
- [26] L. Ling, Y. Zhou, J. Huang, Q. Yao, G. Liu, P. Zhang, W. Sun, W. Wu, Carboxylate-terminated double-hydrophilic block copolymer as an effective and environmental inhibitor in cooling water systems, *Desalination*, 304 (2012) 33–40.
- [27] D. Liu, W. Dong, F. Li, F. Hui, J. Lédion, Comparative performance of polyepoxysuccinic acid and polyaspartic acid on scaling inhibition by static and rapid controlled precipitation methods, *Desalination*, 304 (2012) 1–10.
- [28] Y. Tang, W. Yang, X. Yin, Y. Liu, P. Yin, J. Wang, Investigation of CaCO_3 scale inhibition by PAA, ATMP and PEPEMP, *Desalination*, 228 (2008) 55–60.
- [29] Y. Xu, B. Zhang, L. Zhao, Y. Ciu, Synthesis of polyaspartic acid/5-aminoorotic acid graft copolymer and evaluation of its scale inhibition and corrosion performance, *Desalination*, 311 (2013) 156–161.
- [30] C. Fu, Y. Zhou, G. Liu, J. Huang, W. Sun, W. Wu, Inhibition of $\text{Ca}_3(\text{PO}_4)_2$, CaCO_3 and CaSO_4 precipitation for industrial recycling water, *Ind. Eng. Chem. Res.*, 50 (2011) 10393–10399.
- [31] S.P. Gopi, V.K. Subramanian, Polymorphism in CaCO_3 – effect of temperature under the influence of EDTA (di sodium salt), *Desalination*, 207 (2012) 38–47.
- [32] P. Kjellin, X-ray diffraction and scanning electron microscopy studies of calcium carbonate deposited on a steel surface, *Colloids Surf., A*, 212 (2003) 19–26.
- [33] G. Wolf, E. Königsberger, H.G. Schmidt, I.-C. Königsberger, H. Gamsjäger, Thermodynamic aspects of the vaterite-calcite phase transition, *J. Therm. Anal. Calorim.*, 60 (2000) 463–472.
- [34] K. Sawada, The mechanism of crystallization and transformation of calcium carbonates, *Pure Appl. Chem.*, 69 (1997) 921–928.
- [35] L. Liu, A. He, Research progress of scale inhibition mechanism, *Adv. Mater. Res.*, 955–959 (2014) 2411–2414.
- [36] D.S. Kim, K.C. Lee, Surface modification of precipitated calcium carbonate using aqueous fluorsilicic acid, *Appl. Surf. Sci.*, 202 (2002) 15–23.
- [37] A.A. Al-Hamzah, C.P. East, W.O.S. Doherty, C.M. Fellows, Inhibition of homogeneous formation of calcium carbonate by poly(acrylic acid). The effect of molar mass and end-group functionality, *Desalination*, 338 (2014) 93–105.
- [38] G. Zhang, J. Ge, M. Sun, B. Sun, B. Pan, T. Mao, Z. Song, Investigation of scale inhibition mechanisms based on the effect of scale inhibitor on calcium carbonate crystal forms, *Sci. China B*, 50 (2007) 114–120.
- [39] J. Loiseau, N. Doërr, J.M. Suau, J.B. Egraz, M.F. Llauro, C. Ladavière, Synthesis and characterization of poly(acrylic acid) produced by RAFT polymerization. Application as a very efficient dispersant of CaCO_3 , kaolin, and TiO_2 , *Macromolecules*, 36 (2003) 3066–3077.
- [40] R. Greenwood, Review of the measurement of zeta potentials in concentrated aqueous suspensions using electroacoustics, *Adv. Colloid Interface Sci.*, 106 (2003) 55–81.
- [41] W. Li, G. Zhang, J. Ge, P. Liu, Effects of phosphonates on zeta potential of calcium carbonate, *Jingxi Shiyou Huagong Jinzhan*, 6 (2005) 18–20; cited by Chem. Abstr.